CHAPTER IV

RESULTS AND DISCUSSION

This chapter was divided into 3 parts. The first part concentrated on the synthesis and characterization of negatively charged chitosan, N-sulfofurfuryl chitosan (SFC) and positively-charged chitosan, N-[(2-hydroxyl-3-trimethylammonium)propyl]chitosan chloride (HTACC). The ability of SFC and HTACC as well as unmodified chitosan to form multilayer thin film was determined and explained in the second part. And the last part was dedicated to the evaluation of alternating bioactivity of the assembled multilayer film against a number of selected proteins having different charge and size.

4.1 Synthesis of Charged Derivatives of Chitosan

4.1.1 Synthesis of N-Sulfofurfuryl Chitosan (SFC)

N-sulfofurfuryl chitosan or SFC, the negatively charged derivative of chitosan, was synthesized by reductive alkylation between amino groups (NH_2) of chitosan and 5-formyl-2-furansulfonic acid, sodium salt at room temperature *via* Schiff's base under mild condition. ^1H NMR signals of two furan protons at 6.3 and 6.7 ppm in Figure 4.1 confirmed the attachment of the heterocyclic component. Furthermore, there was a new signal appearing approximately at 4.4 ppm corresponding to the two protons of methylene group that links between the amino group of chitosan and the furan ring. However, the signal could not be clearly observed when the low equivalent of FFSA to amino groups was used. A signal from aldehyde proton of FFSA at 9.5 ppm was not observed in all spectra indicating that there was no FFSA residue left in SFC. The chemical equation of reductive alkylation between chitosan and FFSA was shown in Scheme 2.3.
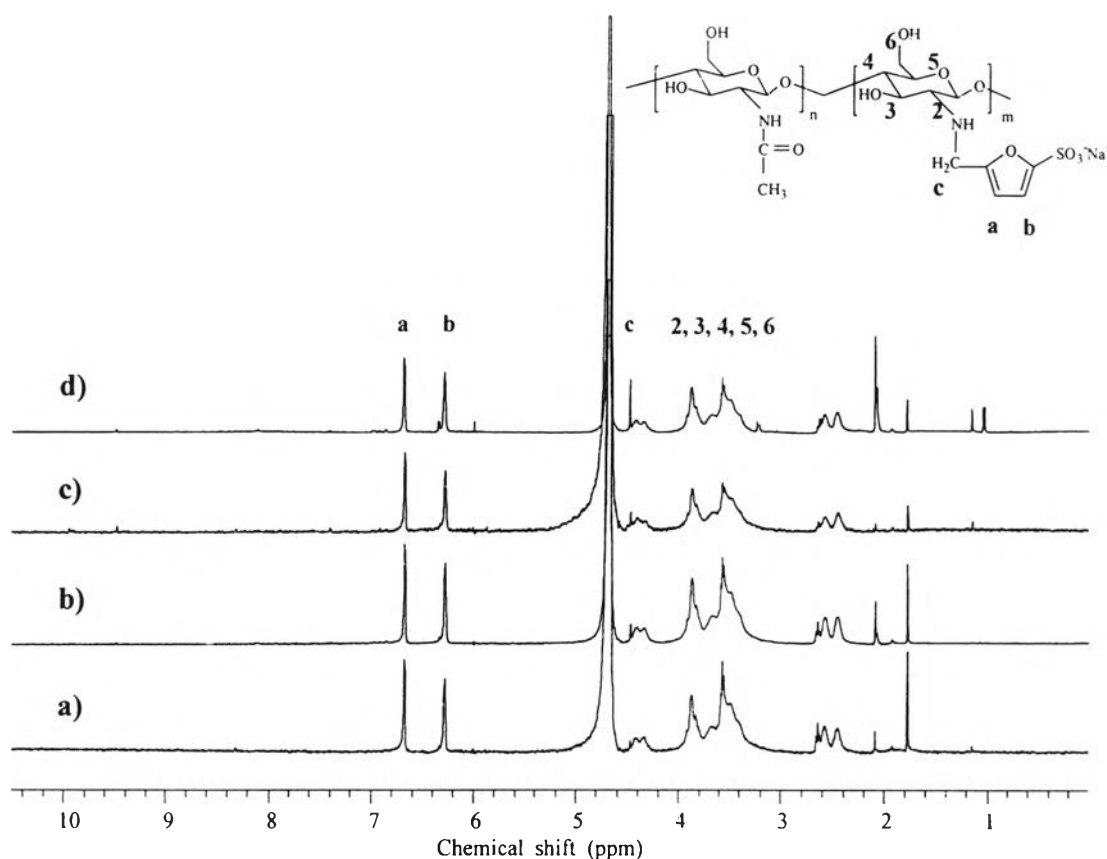
Figure 4.1 ^{1}H NMR spectra of SFC obtained using the mole ratio between FFSA and NH$_2$ of chitosan of a) 0.7, b) 1, c) 2, and d) 4 (solvent: D$_2$O, 25 °C).

Using equation 4.1, %DS of sulfonate group, can be determined by the relative ratio between the peak integration of the two protons of furan group and the peak integration of the proton H-2 to H-6 of chitosan (chemical shift 3.1-4.1 ppm). From Table 4.1, %DS of sulfonate group on chitosan was apparently elevated from 48 to 63 when the FFSA equivalent was increased from 0.7 to 2. %DS was not much further increased using 4 equivalent of FFSA, therefore, 2 equivalent of FFSA was suggested as the optimal ratio for preparation of SFC to be used for multilayer assembly.

$$\%DS = \{[H\text{-}a, H\text{-}b] \times 1/2\} / \{[H\text{-}2, 3, 4, 5, 6] \times 1/5\} \times 100 \qquad (4.1)$$

Table 4.1 Degree of substitution (%DS) of sulfonate group on chitosan after reacting with FFSA in acetic acid/MeOH (1:1, v/v) for 18 h as determined by ^{1}H-NMR.

Equivalent of FFSA	Integration		%DS
	[H] from H-2,3,4,5,6 of chitosan	[CH] from =CH – CH= of furan	
0.7	8.8	1.7	48
1	8.1	1.6	49
2	8.4	2.0	60
4	8.0	2.0	63

For comparison, FT-IR spectra of chitosan and FFSA were displayed together with the one of SFC. The appearance of peaks at 1233 cm^{-1} of O=S-O stretching and 1040 cm^{-1} of S=O stretching in FT-IR spectrum of SFC signified the presence of the sulfonate salt and sulfonic acid functionality, respectively.
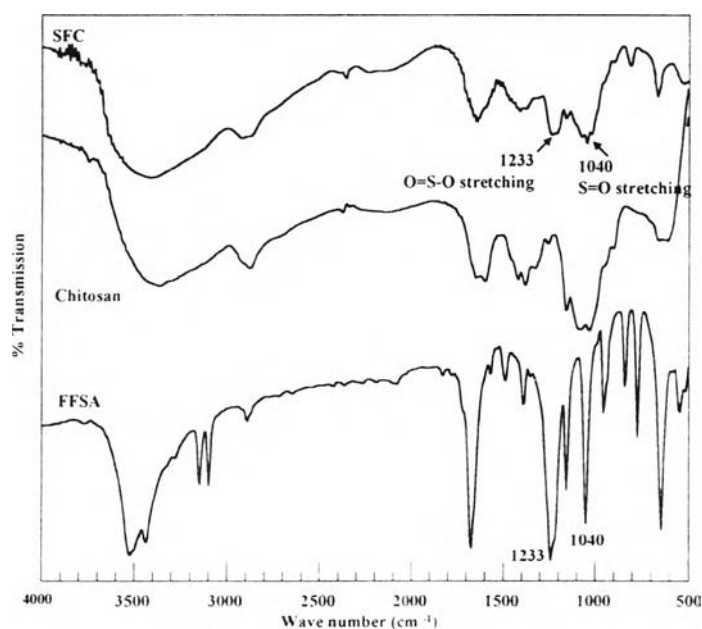

Figure 4.2 FT-IR spectra of FFSA, chitosan and SFC.

4.1.2 Synthesis of *N*-[(2-hydroxyl-3-trimethylammonium)propyl]chitosan chloride (HTACC)

N-[(2-hydroxyl-3-trimethylammonium)propyl]chitosan chloride or HTACC, the positively charged derivative of chitosan was synthesized by epoxide ring opening of glycidyltrimethylammonium chloride (GTMAC) by amino groups of chitosan under acidic condition. In theory, GTMAC mainly reacts with amino (NH_2) groups under acidic condition but preferably reacts with hydroxyl (OH) groups under neutral and alkaline condition. The acidic condition causes protonation at oxygen and makes the epoxy ring of GTMAC more reactive towards the NH_2 groups of chitosan. Figure 4.3 illustrates ^1H NMR spectra of the synthesized HTACC. Signals corresponding to the protons of CH_2 and CH appeared at 2.6 and 4.4 ppm, respectively. Furthermore, there is a new strong CH_3 peak at 3.1 ppm, indicating that the quaternary ammonium group of $N^+(CH_3)_3$ was incorporated.
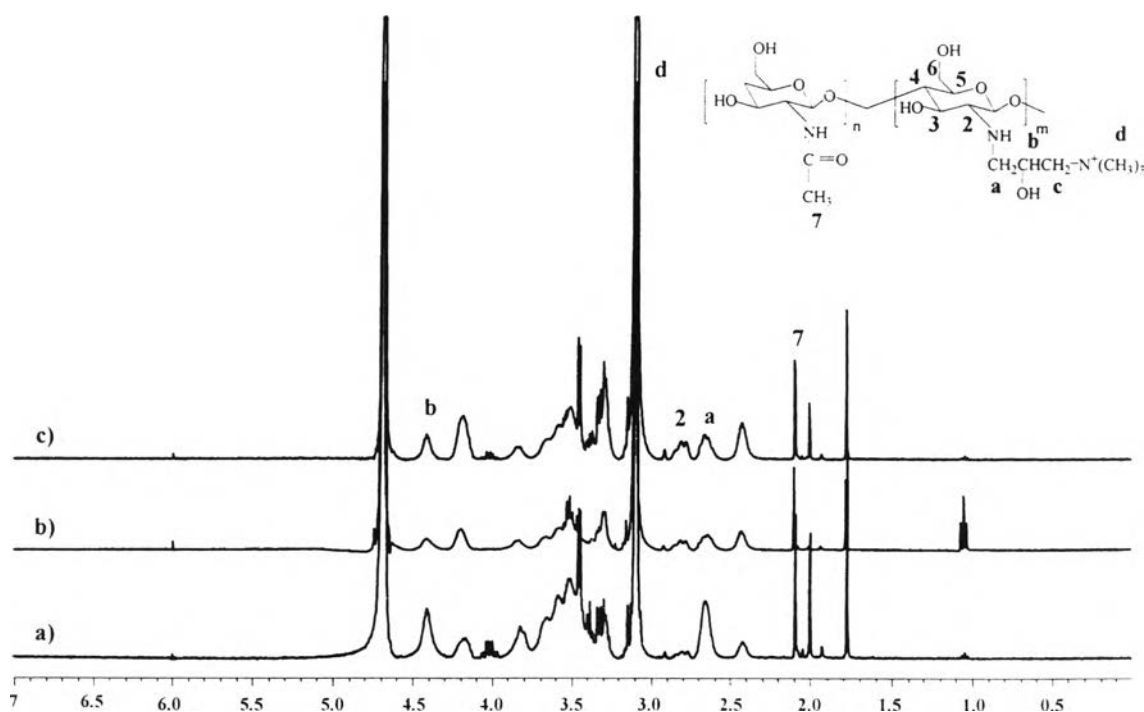

Figure 4.3 ^1H NMR spectra of HTACC obtained using the mole ratio between GTMAC and NH_2 of chitosan of a) 2, b) 4, and c) 6 (solvent: D_2O, 25 °C).

%DS of GTMAC on chitosan was calculated from the relative ratio between the peak integration of proton from the quaternary ammonium group at 3.1 ppm of GTMAC and the methyl protons of acetamide group at 2.1 ppm of chitosan [12] using equation 4.2. It should be noted that the amount of methyl protons in acetamide group could be relatively determined from %DD of chitosan which is 95% in this case. From Table 4.2, %DS of quaternary ammonium group on chitosan was drastically increased from 49 to 96 when the GTMAC equivalent was increased from 2 to 4. %DS was not much further increased using 6 equivalent of FFSA, 4 equivalent of GTMAC was therefore suggested as the optimal ratio for preparation of HTACC to be used for multilayer assembly.

$$\%DS = \{[H\text{-}d]/9\} / \{[H\text{-}7]/3\} \times 5/100 \times 100 \qquad (4.2)$$

Table 4.2 Degree of substitution (%DS) of quaternary ammonium group on chitosan after reacting with GTMAC at 70 °C in acetic acid for 24 h as determined by ^{1}H-NMR.

Equivalent of GTMAC	Integration		%DS
	H-7 of chitosan	H-d of GTMAC	
2	0.2	5.9	49
4	0.5	28.8	96
6	0.5	30.6	100

The success of HTACC synthesis could also be verified by the decrement of the N-H scissoring peak at 1599 cm^{-1} of amino groups of chitosan and the appearance of C-H bending peak at 1482 cm^{-1} corresponding to the methyl groups of quaternary ammonium groups as shown in Figure 4.4.
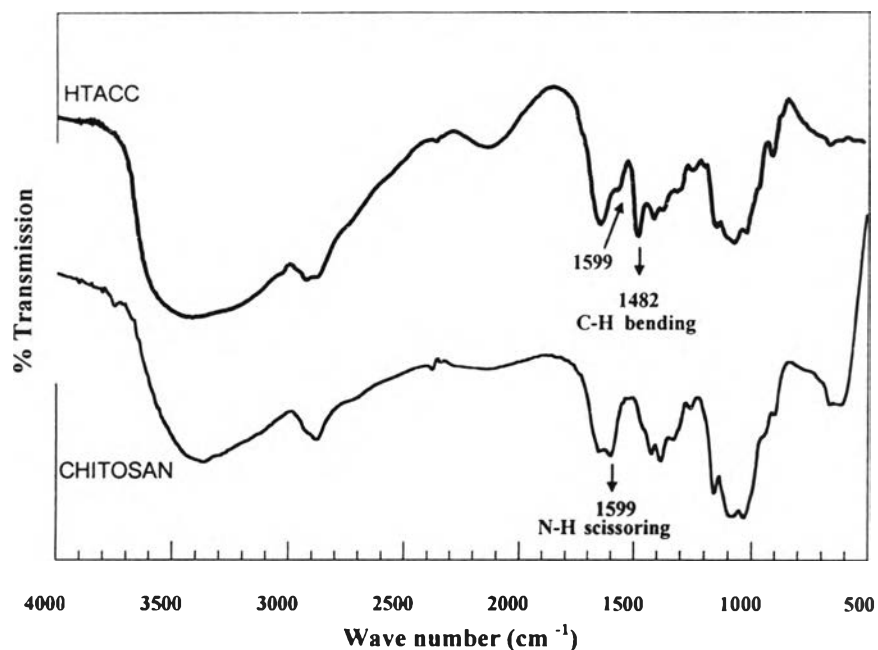
Figure 4.4 FT-IR spectra of chitosan and HTACC.

4.1.3 Solubility of SFC and HTACC

The solubility test was performed according to a method of Hitoshi *et al* [7]. Solid sample of charged derivative of chitosan (60 mg) was dissolved in water (20 mL). The pH of the solution was adjusted with 0.5% w/v aqueous HCl and NaOH. SFC showed the solubility only in the alkaline region range (pH 8-13), and the insolubility in the acidic (pH < 7) and the neutral region (pH 7). In contrast, HTACC having quaternary ammonium groups showed the solubility in the entire pH range.

4.1.4 Adsorption of Charged Derivatives of Chitosan

4.1.4.1 Effect of Adsorption Time and Concentration

To select the adsorption time at which adsorption of each polyelectrolyte has reached its equilibrium, *in-situ* monitoring of adsorption was operated using QCM measurement. One side of the quartz crystal was in permanent contact with polyelectrolyte solution and the frequency change was recorded continuously. Figure 4.5 showed frequency shift of quartz crystal due to SFC adsorption. The greater frequency shift was observed when the higher concentration of SFC was used. The similar trend was also realized for the adsorption of HTACC. Such a trend may stem from the fact that the higher polyelectrolyte concentration generally promotes the physical adsorption in multilayer fashion which does not persist after the thorough rinsing is applied. As a result, the magnitude of frequency change shown in Figure 4.5 should not correspond with the actual quantity of polyelectrolyte that adsorbed on the quartz crystal because rinsing was not applied in the experiment. According to the data displayed in Table 4.3, the adsorption seemed to reach saturation in about 30 minutes, the period of time later used for multilayer assembly.

According to the adsorption isotherms of SFC and HTACC shown in Figure 4.6, the concentration of 2 mg/mL and 3 mg/mL seemed to be sufficient for SFC and HTACC to reach its adsorption equilibrium, respectively.
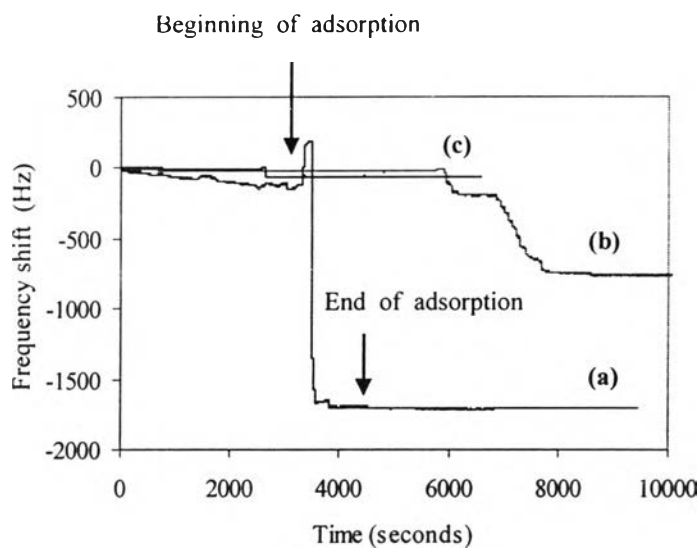
Figure 4.5 *In situ* monitoring of frequency shift (Hz) as a function of time of SFC without NaCl at pH 8 having different concentration: (a) 3 mg/mL, (b) 2 mg/mL, and (c) 1 mg/mL.

Table 4.3 Frequency shift (Hz) and adsorption time at equilibrium (min) of SFC and HTACC obtained from *in-situ* monitoring by QCM.

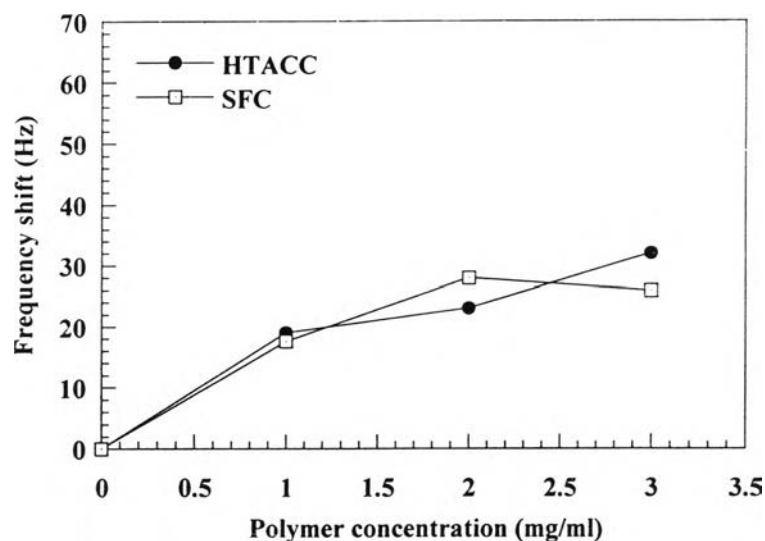| Polyion and concentration	Frequency shift, ΔF (Hz)	Adsorption time (min)
1 mg/mL of SFC	56	7
2 mg/mL of SFC	747	23
3 mg/mL of SFC	1580	4
1 mg/mL of HTACC	169	29
2 mg/mL of HTACC	453	29
3 mg/mL of HTACC	1219	17

Figure 4.6 Adsorption isotherms of SFC and HTACC determined by conventional mode of QCM.

4.1.4.2 Effect of Ionic Strength

The effect of ionic strength on the polyelectrolyte adsorption was studied using QCM measurement in conventional mode. Frequency changes due to adsorption were measured in air after immersing the quartz crystal in polyelectrolyte solution for 30 min, washing and drying. Frequency shift shown in Table 4.4 indicates that the amount of polyelectrolyte adsorption increased when NaCl was added. This result can be explained by the fact that polyelectrolyte tends to adopt coil-like conformation in the presence of NaCl due to a relaxation of intra-chain and inter-chain electrostatic repulsion in polymer solution. The adsorbed layer of coil-like polyelectrolyte was therefore thicker than one of polyelectrolyte that favorably exists in the extended form in the absence of NaCl.

Table 4.4 Frequency shift (Hz) after adsorption of SFC and HTACC measured by conventional mode of QCM.

Polyions	NaCl (M)	Frequency shift, ΔF (Hz)
2 mg/mL of SFC	0	28
2 mg/mL of SFC	1.0	127
3 mg/mL of HTACC	0	32
3 mg/mL of HTACC	1.0	145

4.2 Alternative Layer-by-layer Adsorption

4.2.1 Confirmation of Multilayer Formation

QCM was used to confirm the multilayer formation by monitoring frequency change as a function of a number of deposition. Progressive increase of QCM frequency with a number of deposition step (shown in Figure 4.7) evidently indicated stepwise deposition of all three polycation-polyanion pairs (chitosan-PSS, PAH-SFC and HTACC-PAA). It was assumed that the thickness of each layer corresponded with the amount of adsorbed polymer which can be directly calculated from the frequency change. The frequency change associated with the thickness of multilayer film built up from HTACC and PAA was the lowest. This can be explained as a consequence of HTACC as a strong polyelectrolyte being adsorbed first as a thin layer. At pH 7, the second layer adsorption was mainly driven by electrostatic attraction between NH_3^+ group of HTACC and COO^- group of PAA yielding a relatively thin layer of HTACC. Although PAA is a weak polyelectrolyte, its adsorption depends strongly on the thickness of the first deposit layer of HTACC at neutral pH where COOH groups are essentially ionized to COO^- groups. At pH 4, chitosan which is a weak polycation bears

both NH_3^+ and NH_2. The adsorption of PSS which is a strong polyelectrolyte was driven by both electrostatic attraction between NH_3^+ groups and SO_3^- groups and hydrogen bonding between SO_3^- and some NH_2 groups of chitosan. As a result, the overall layers of chitosan-PSS pair seemed to be thicker than HTACC-PAA pair. The situation for chitosan-PSS pair is quite similar to that for HTACC-PAA pair due to two facts: (1) the stepwise adsorption occurs between a pair of strong and weak polyelectrolytes, (2) the adsorption is mainly driven by electrostatic interaction. For that reason, the overall thickness of multilayer assembled from chitosan and PSS was not much larger than the one of multilayer assembled from HTACC and PAA. Unlike other two polyelectrolyte pairs, the increment of frequency change due to PAH and SFC deposition are unexpectedly high suggesting that the relatively thick multilayer film was formed. As a result of incomplete substitution of N-sulfofurfuryl groups at NH_2 position of chitosan, SFC bears both SO_3^- and NH_2 groups. At pH 8, the adsorption of SFC on PAH layer and vice versa was then controlled by both electrostatic interaction and H-bonding. The unique combination of PAH and SFC then gave rise to the presumably thick multilayer.
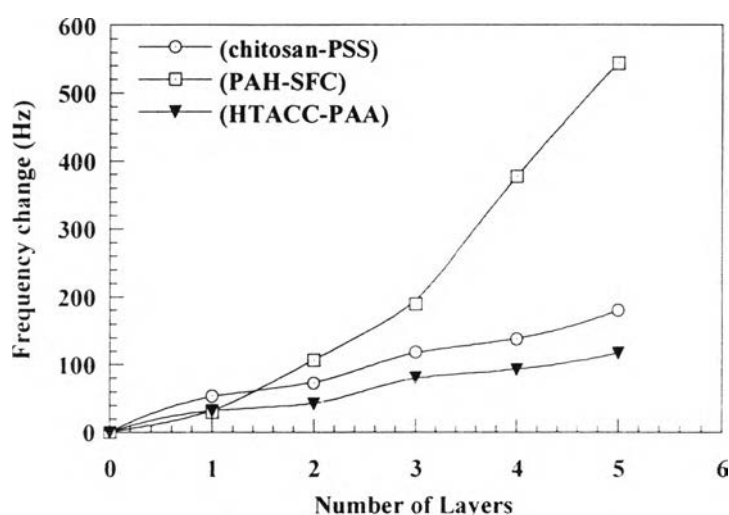

Figure 4.7 Frequency change obtained from QCM analysis as a function of a number of layer.

4.2.2 Multilayer Assembly

Up to now, most studies on polyelectrolyte multilayers have been accomplished on silicon or glass substrates. Due to a focus on future biomedical applications, studying polyelectrolyte multilayer on polymeric substrates appears increasingly important. Since conventional polymers are usually uncharged, surface pretreatment is necessary to generate charged groups on polymer surface. In this study, plasma-treated PET, a polymeric substrate bearing hydroxyl and carboxyl groups on the surface, was used as a substrate for multilayer formation. The pre-treatment caused the water contact angle of the plasma-treated PET surface to drop from 67° to about 53°.
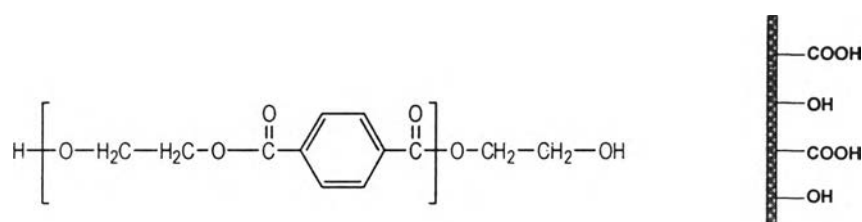

Figure 4.8 Chemical structures of PET (left) and plasma-treated PET (right).

In this section, multilayer assembly of three pairs of polycation-polyanion on plasma-treated PET substrates in the presence of 1M NaCl was investigated (chitosan-PSS at pH 4, PAH-SFC at pH 8 and HTACC-PAA at pH 7). Chemical structures of all polyelectrolytes are illustrated in Figure 4.9.
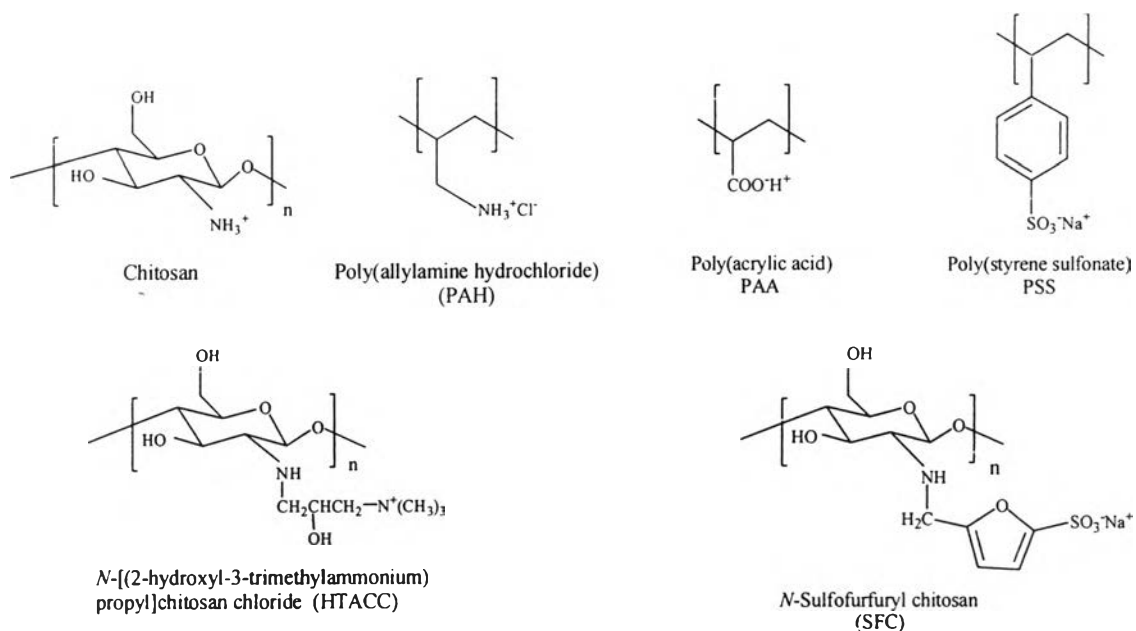
Figure 4.9 Polycations and polyanions used for multilayer assembly.

For PET substrate, which showed a negatively charged surface at appropriated pH, the first adsorption cycle was carried out in polycation solution (chitosan, PAH or HTACC). The plasma-treated PET should be able to adsorb polycation *via* ionic interactions between $-COO^-$ and $-NH_3^+$ or H-bonding between $-OH$ and $-NH_2$. If the total number of layer is odd, the last layer adsorbed is polycation. And if the total number of layer is even, the last layer adsorbed is polyanion.

4.2.3 Stratification of Multilayer Film

If the concept of alternative adsorption is valid, the surface property of the multilayer film should alternatively change. In other words, the multilayer film should be stratified. Water contact angle data shown in Figure 4.10 confirmed that the assembled film was stratified. The number appearing on the horizontal scale of represented the number of deposition. If the number of layer is odd, the charge of the outermost layer is positive. If the number of layer is even, the charge of the outermost layer is negative. Each individual layer should be relatively thicker than the sampling

depth of contact angle measurement (a few Angstrom) so that the wettability of the multilayer film was strongly dependent on the last layer deposited and the influence of the underlying layers was not observed. The assembled film having the odd number of deposited layer (positively-charged surface) was clearly more hydrophobic than the one having the even number of deposited layer (negatively-charged surface).
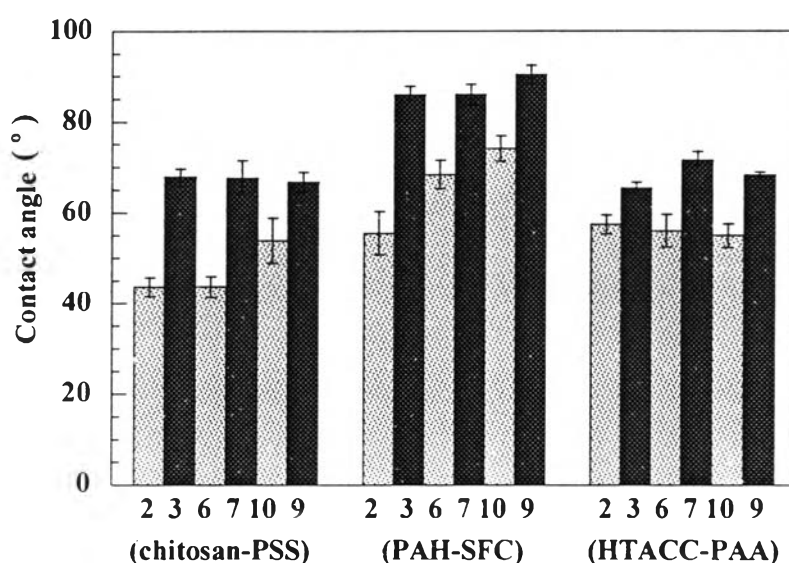

Figure 4.10 Water contact angles of the multilayer thin film.

ATR-IR technique was used to characterize function groups of multilayer film. Figure 4.11 displays ATR-IR spectra of multilayer films. The absence of new signals that are characteristic peaks of polyelectrolytes in all samples implied that the thickness of multilayer may not reach the sampling depth of ATR-IR technique which is in the range of 1-2 µm. The larger number of deposition is definitely required to be able to detect the existence of adsorbed multilayer film.
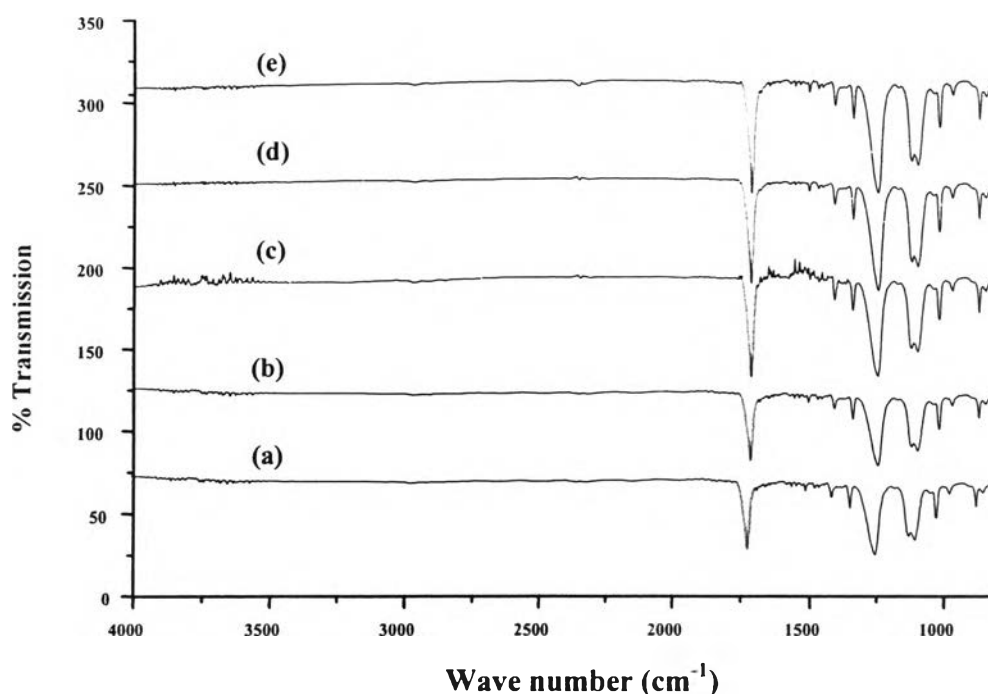
Figure 4.11 ATR-IR spectra of treated PET and multilayer films: (a) treated PET-(HTACC-PAA)$_{13}$, (b) treated PET-(HTACC-PAA)$_{12}$-HTACC, (c) treated PET-(chitosan-PSS)$_{13}$, (d) treated PET-(chitosan-PSS)$_{12}$-chitosan, and (e) treated PET

4.3 Protein Adsorption

Biocompatibility of the assembled films was determined in terms of protein adsorption. The proteins used in this investigation include albumin, fibrinogen, lysozyme and γ-globulin whose physical properties are listed in Table 4.5. All proteins are varied in size, charge as well as conformational stability under the experimental condition (pH 7.4). The amount of protein adsorption on the multilayer film surface was determined by bicinchoninic acid (BCA) assay. A calibration curve using albumin as a standard is displayed in Appendix B.

Table 4.5 Physical properties of proteins used in this investigation

Physical Property	Albumin	Fibrinogen	γ-Globulin	Lysozyme
Mass (Da)	69,000	340,000	165,000	14,600
Isoelectric point (pH units)	4.8	5.5	6.5	11.1

Adsorption of albumin (BSA) on multilayer films was shown in Figure 4.12. Albumin protein is a carboxylic acid-rich protein. Its carboxylic acid group is converted to a negatively charged carboxylate ion at pH 7.4. As expected, the adsorbed amount of BSA on the multilayer having the odd number of layer (7 and 9) and positive charge was higher that the one having the even number of layer (6 and 10) and negative charge. Such a trend can be explained by the fact that the adsorption was promoted by electrostatic attraction between the positively-charged surface of the outermost layer and BSA. On the other hand, the adsorption of negatively charged BSA was suppressed on the negatively charged surface having PSS, SFC or PAA as the top layer due to the electrostatic repulsion.
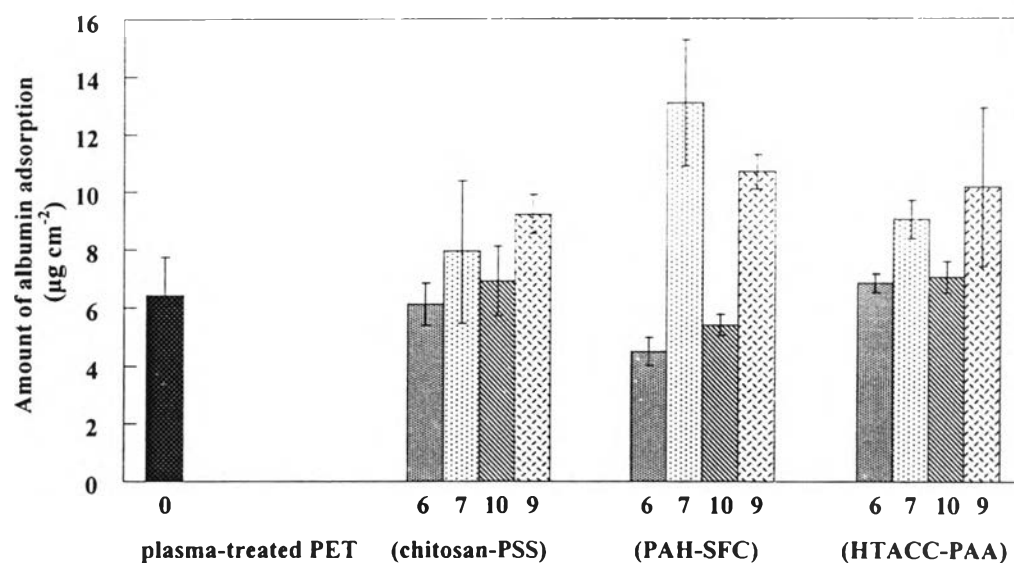
Figure 4.12 The amount of BSA adsorption per surface area ($\mu g/cm^2$) of treated PET, (chitosan-PSS)$_n$, (PAH-SFC)$_n$, and (HTACC-PAA)$_n$ assemblies on treated PET substrates in the presence of 1M NaCl.

Similar to albumin, fibrinogen (FIB) exhibited an adsorption trend in alternate fashion corresponding with the surface charge of multilayer film. The significantly high quantity of adsorbed BSA in comparison with the one of adsorbed FIB is due in large part to the variation in size of protein. Not only can BSA, as a small protein, adsorb on the top surface, it may also absorb inside the top layer. This may be the reason why odd-even effect of BSA adsorption was not so strong in the cases of chitosan-PSS and HTACC-PAA whose individual layer is quite thin. It is most likely that the adjacent underlying layer having the opposite charge to the top layer plays a part in adsorption. The closer to the interface of the top layer/the adjacent underlying layer, the lesser the charge density. Under such circumstance, the influence of charge characteristic of the top layer on protein adsorption becomes weak. Because the assumed permeation into the top layer of the assembled film was somewhat limited for the large protein like FIB, the odd-even effect was quite significant independent of the system.
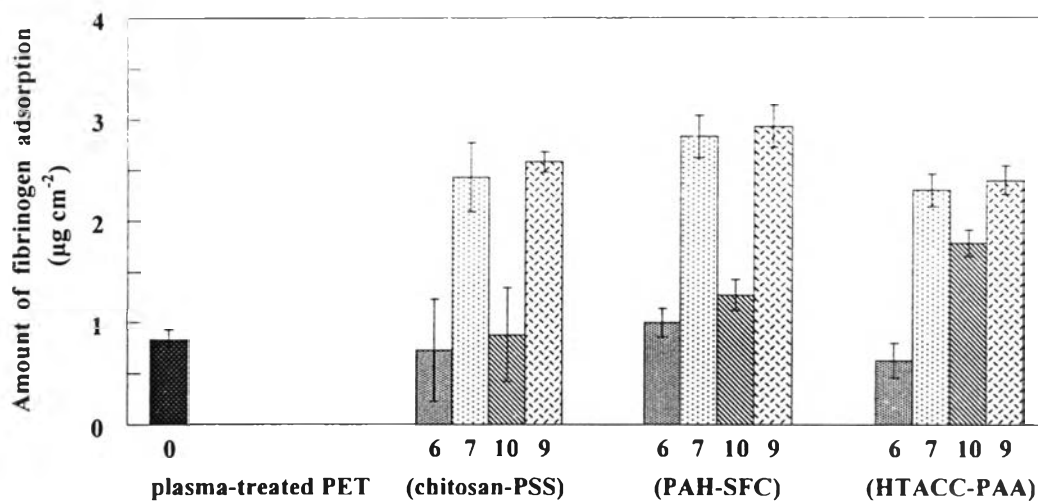
Figure 4.13 The amount of FIB adsorption per surface area ($\mu g/cm^2$) of treated PET, $(chitosan-PSS)_n$, $(PAH-SFC)_n$, and $(HTACC-PAA)_n$ assemblies on treated PET substrates in the presence of 1M NaCl.

With a pI value of 6.5, γ-globulin (GLB) should be positive in charge at pH 7.4. In comparison with BSA and FIB, GLB should exhibit its adsorption in a reverse manner. The data shown in Figure 4.14 indicated that it is not the case for three systems. Having pI very close to 7.4, GLB may not be strongly charged. As a result, electrostatic interaction is no longer a major driving force for adsorption. It is thus believed that the weakly charge and the moderate size of GLB are responsible for the absence of odd-even effect.

Lysozyme (LYZ) is selected as another positively-charged protein for adsorption study. LYZ is quite a small protein having the lowest mass among all studied proteins. The amount of adsorbed LYZ per surface area has reached as high as 30 $\mu g/cm^2$. The expected alternate adsorption was observed on PAH-SFC and HTACC-PAA systems. The enzymatic activity of LYZ towards chitosan perhaps account for peculiar trend in the chitosan-PSS system.
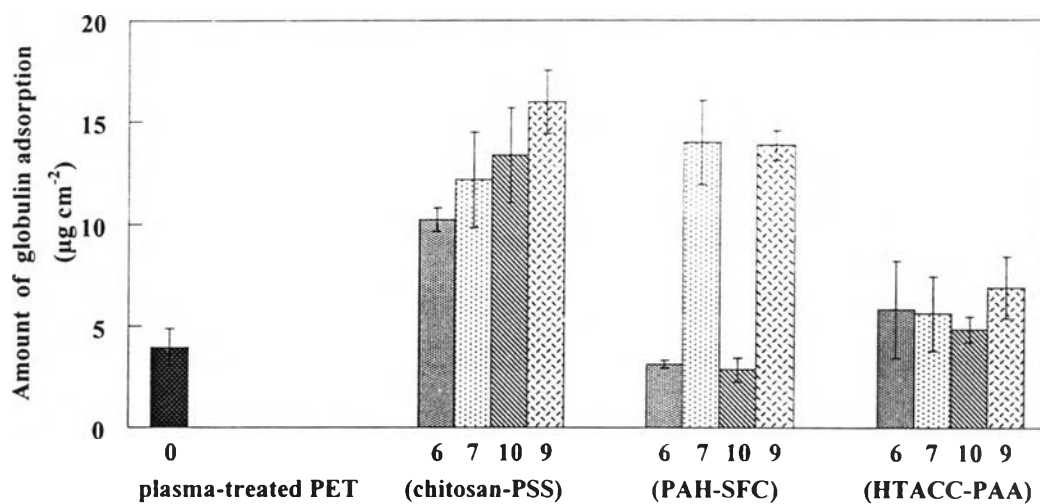
Figure 4.14 The amount of GLB adsorption per surface area ($\mu g/cm^2$) of treated PET, (chitosan-PSS)$_n$, (PAH-SFC)$_n$, and (HTACC-PAA)$_n$ assemblies on treated PET substrates in the presence of 1M NaCl.

Figure 4.15 The amount of LYZ adsorption per surface area ($\mu g/cm^2$) of treated PET, (chitosan-PSS)$_n$, (PAH-SFC)$_n$, and (HTACC-PAA)$_n$ assemblies on tr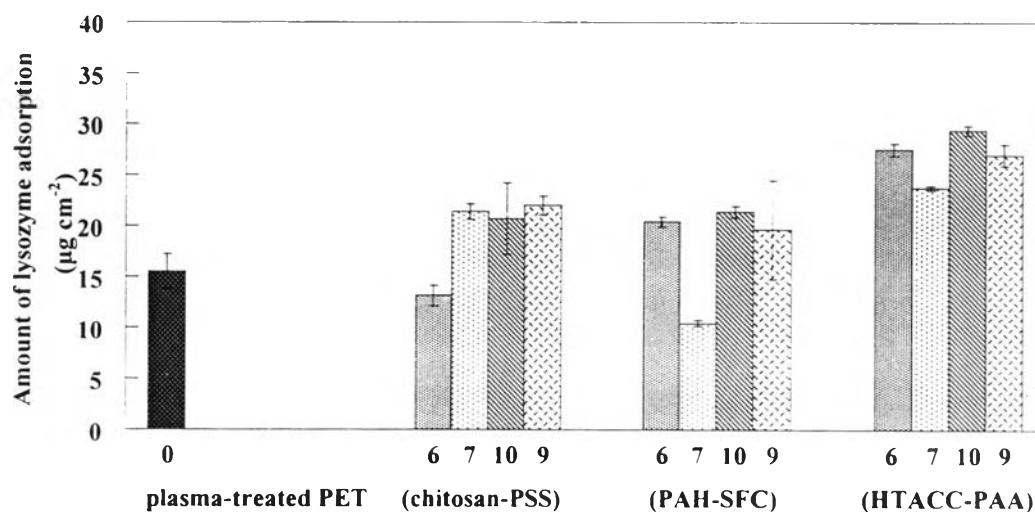eated PET substrates in the presence of 1M NaCl.